Strongly localized molecular orbitals for α-quartz

2004 J. Phys.: Condens. Matter 16 7233

(http://iopscience.iop.org/0953-8984/16/41/006)

INSTITUTE OF PHYSICS PUBLISHING JOURNAL OF PHYSICS: CONDENSED MATTER

J. Phys.: Condens. Matter **16** (2004) 7233–7246 PII: S0953-8984(04)81040-3

Strongly localized molecular orbitals for α-quartz

Oleh Danyliv[1] **and Lev Kantorovich**

Department of Physics, Kings College London, Strand, London WC2R 2LS, UK

E-mail: oleh.danyliv@kcl.ac.uk

Received 20 May 2004, in final form 9 August 2004
Published 1 October 2004
Online at stacks.iop.org/JPhysCM/16/7233
doi:10.1088/0953-8984/16/41/006

Abstract

A previously proposed computational procedure for constructing a set of non-orthogonal strongly localized one-electron molecular orbitals (Danyliv and Kantorovich 2004 *Phys. Rev.* B **70** 075113) is applied to a perfect α-quartz crystal characterized by an intermediate type of chemical bonding. The orbitals are constructed by applying various localization methods to canonical Hartree–Fock (HF) orbitals calculated for a succession of finite molecular clusters of increased size with appropriate boundary conditions. The calculated orbitals span the same occupied Fock space as the canonical HF solutions, but have the advantage of reflecting the true chemical nature of the bonding in the system. The applicability of several localization techniques as well as a number of possible choices of localization regions (structure elements) are discussed for this system in detail.

(Some figures in this article are in colour only in the electronic version)

1. Introduction

Quantum cluster embedding [1–6] has become a powerful computational tool in the electronic structure theory of extended systems, such as large biological molecules [7, 1, 8, 9, 2], surface defects and adsorption on crystal surfaces [10–12] or point defects in the bulk of crystalline [13, 14] or amorphous [15] systems. The embedding methods originate from a model in which a single local perturbation is considered in the direct space of the entire system inside a *finite* quantum molecular cluster in great detail, whereas a more approximate method is used to account for the rest of the system surrounding the cluster.

We believe that the formalism based on group functions is the most appropriate one for the derivation of any embedding scheme. The method based on overlapping (not strongly orthogonal) group functions [16, 17] is presently being developed in our laboratory. Our method, which is similar in spirit to some one-electron methods [18–20], is based on the

[1] On leave from: Institute for Condensed Matter Physics, National Academy of Science of Ukraine, Ukraine.

construction of strongly localized orbitals which are designed to represent the true electronic density of the entire system via a combination of elementary densities associated in simple cases with atoms, ions and/or bonds. Our initial effort in this project is focused on the development of an embedding scheme based on the Hartree–Fock (HF) approximation and applied to point defects in the bulk or at surfaces of periodic crystals. The next step would be the implementations of the group functions approach to density functional theory. Construction of the overlapping (not orthogonal) strongly localized molecular orbitals (LMOs) as building blocks of the entire system is crucial for this technique. The LMOs are designed to represent the true electronic density of reference systems (such as, for example, 3D ideal perfect crystals or 2D periodic crystal surfaces) and are constructed to have transparent chemical meaning, for example to represent ions in the case of ionic systems and covalent bonds in covalently bound systems. Although we are not yet concerned in this study with biological systems which do not possess periodicity, we note that most of the ideas of our method can also be applied to these systems as well.

A convenient and simple method for calculating the LMOs for 3D periodic systems (e.g. perfect crystals) was recently suggested in [21]. This method is based on finding appropriate linear combinations of the canonical HF solutions for a sequence of finite molecular clusters of increased size. The linear combinations are chosen in such a way as to optimize special *localizing functionals* constructed to obtain orbitals localized within certain *regions* (e.g. bonds, atoms, ions, etc). There may be several different regions in every unit cell of the crystal.

The method was successfully applied in [21] to two cases of extreme ionic (MgO crystal) and covalent (Si crystal) bonding. In both cases four LMOs were found in every unit cell. In the former case every unit cell is composed of a single region which is associated with an oxygen ion; the region contains eight electrons and is described by four mutually orthogonal LMOs. In the latter case (the Si crystal) every unit cell is represented by four neighbouring regions. Each region is associated with a pair of nearest Si atoms, contains two electrons and is described by a single double occupied LMO. The four regions belonging to the same unit cell have one common Si atom at the centre of a tetrahedron and the other four Si atoms form its vertices. The four LMOs within the same cell do overlap and thus are not orthogonal.

The main purpose of this paper is to check if our method [21] can be extended to systems which have more complicated types of chemical bonding. This is invaluable for the future development of our embedding method towards describing insulating crystals with arbitrary type of bonding. Therefore, we here consider in detail the α-quartz (SiO_2) crystal, which may be thought of as a prototype system with an intermediate (ionic–covalent) type of chemical bonding. Essentially two main questions are addressed here with respect to the localization of the calculated LMOs: (i) the choice of regions and (ii) the choice of localization methods (i.e. the localization functionals).

The plan of the paper is the following. In the next section the main ideas of our method are briefly described (for the full discussion, see [21]). Three localization methods are introduced (one of them was not used in our previous study [21]) alongside a choice of three localization criteria. Application of our method to the α-quartz crystal is considered in section 3. Brief conclusions are given in section 4.

2. Localization procedure

2.1. General approach

Let us assume that we know an occupied canonical set of one-electron molecular orbitals, $\{\varphi_i^c(\mathbf{r})\}$, for a perfect 3D periodic crystal. These orbitals may be obtained as eigenvectors

of the appropriate Hartree–Fock (HF) problem using, for example, the CRYSTAL code [22] which employs the periodic symmetry directly. In our method, however, we consider instead a specially designed set of *finite* clusters of increased size and find the HF solutions for them using one of the available quantum chemistry packages. It was demonstrated in [21] that this approach is equivalent to using a periodic-crystal electronic structure approach as far as the LMOs are concerned, provided that large enough molecular clusters are used.

The canonical molecular orbitals (CMOs) are orthogonal and span the entire occupied Fock space. They are not localized in space, and have a non-zero contribution on atoms of every unit cell in the crystal. In practice, when the cluster method is employed, they span the entire cluster. In other words, the CMOs are assumed to be given as a linear combination of the atomic orbitals, $\chi_\mu(\mathbf{r})$, centred on all atoms of the cluster in question:

$$\varphi_i^{\mathrm{c}}(\mathbf{r}) = \sum_\mu C_{\mu i}^{\mathrm{c}} \chi_\mu(\mathbf{r}). \tag{1}$$

In order to describe the crystal as a set of overlapping (non-orthogonal) localized functions, $\{\tilde{\varphi}_a(\mathbf{r})\}$, which span the same occupied Fock space, one has to obtain appropriate linear combinations of the original canonical set $\{\varphi_i^{\mathrm{c}}(\mathbf{r})\}$. In order to do this, it is first necessary to identify *regions* of space where each of the functions $\tilde{\varphi}_a(\mathbf{r})$ has to be localized. Although any (non-singular) linear combination of the canonical set will give the same electron density $\rho(\mathbf{r})$, we adopt here a strategy based on the chemistry of the system in question. Namely, the choice of the localization regions in the first instance is based on the expected type of the chemical bonding in the system: for example, atoms/ions in the cases of atomic/ionic systems, two nearest atoms in the case of covalent bonding, etc. A more complicated choice is anticipated in the cases of intermediate bonding, as will be demonstrated in section 3. Several different nonequivalent regions may be necessary to represent a crystal unit cell which can then be periodically translated to reproduce the whole infinite crystal. Note that several localized orbitals may be associated with each region. For instance, in the case of the Si crystal one needs four localized regions associated with four bonds; each bond is represented by a single double occupied localized orbital and all four bonds have one common Si atom in the centre of the tetrahedron.

Once the localized regions are identified, it is necessary to find linear combination of the CMOs which are localized in each of the regions,

$$\tilde{\varphi}_a(\mathbf{r}) = \sum_j^{\mathrm{occ}} U_{aj} \varphi_j^{\mathrm{c}}(\mathbf{r}) \equiv \sum_\mu \tilde{C}_{\mu a} \chi_\mu(\mathbf{r}). \tag{2}$$

The transformation $\mathbf{U} = \|U_{aj}\|$ of the CMOs within the occupied subspace is arbitrary and, in general, *non-unitary*. In the latter case the expression for the density via the new set of orbitals should contain the inverse of the overlap matrix $\tilde{\mathbf{S}} = \|\tilde{S}_{ab}\|$ [23]:

$$\rho(\mathbf{r}) = 2 \sum_{ab}^{\mathrm{occ}} \tilde{\varphi}_a(\mathbf{r}) (\tilde{\mathbf{S}})_{ab}^{-1} \tilde{\varphi}_b^*(\mathbf{r}) \tag{3}$$

where $\tilde{S}_{ab} = \langle \tilde{\varphi}_a(\mathbf{r}) | \tilde{\varphi}_b(\mathbf{r}) \rangle$ is the overlap integral. The double summation here is performed over all localized orbitals of the whole infinite crystal. If the transformation is unitary, then both the overlap matrix and its inverse are unity matrices and the density takes on its usual 'diagonal' form.

In general, any localization procedure is equivalent to some transformation $\mathbf{U}$ of the CMOs. To find the necessary transformation for, say, region A, an optimization (minimization or maximization) problem is formulated for some specific *localizing functional* $\tilde{\Omega}_{\mathrm{A}}[\{\tilde{\varphi}_a\}]$ with

the constraint that the LMOs associated with region A are orthonormal. This leads to a standard eigenvalue–eigenvector problem:

$$\sum_{j}^{\text{occ}} \Omega_{ij}^{\text{A}} U_{aj} = \lambda_a U_{ai} \tag{4}$$

for the elements of the transformation matrix $\mathbf{U}$. Here Ω_{ij}^{A} is a matrix element of an operator $\hat{\Omega}_{\text{A}}$ calculated using canonical orbitals $\varphi_i^{\text{c}}(\mathbf{r})$. The operator $\hat{\Omega}_{\text{A}}$ is uniquely defined from the functional $\tilde{\Omega}_{\text{A}}[\{\tilde{\varphi}_a\}]$. Although for some localizing functionals (see, e.g. [21]) the matrix elements Ω_{ij}^{A} may depend on the LMOs themselves so that the problem (4) is to be solved self-consistently, we do not consider those functionals in this paper.

Note that LMOs associated with different regions will not be orthogonal in this method. This is because they are obtained from different localizing functionals which strongly depend on the region in question, so that LMOs from different regions are determined by solving different secular problems. For instance, if the LMOs $\{\tilde{\varphi}_a(\mathbf{r})\}$ correspond to region A, then the LMOs $\{\tilde{\varphi}_b(\mathbf{r}) \equiv \tilde{\varphi}_a(\mathbf{r} - \mathbf{L})\}$ are obtained for a physically equivalent region B separated from A by a lattice translation $\mathbf{L}$.

Using a physical argument, each region is associated with a certain *even* number of electrons $2n$. Therefore, if Ω_{A} is minimized, we choose the first n eigenvectors of the problem (4); if, however, Ω_{A} is maximized, the last n solutions are adopted. By collecting LMOs from all regions in the unit cell and then translating those over the whole crystal it should be possible to span the whole occupied Fock space and thus construct the total electron density (3). The larger the finite cluster used while calculating the canonical orbitals, the closer the Fock space will be reproduced by the LMOs.

To summarize, we first suggest a possible set of localization regions in the unit cell and then consider a set of finite molecular clusters (with appropriate boundary conditions) which have all these regions in their central part. Then, we obtain the occupied canonical HF orbitals for each of the clusters using a standard quantum-chemistry package. Out of all the clusters considered, a cluster is chosen for which the electron density is well converged in its central part. Next, using a localization functional, canonical occupied HF orbitals of the chosen cluster are transformed into LMOs. The procedure is repeated for several localization functionals and in each case localization criteria are applied. Then, if necessary, a different choice of localization regions is made, and the whole procedure is repeated. As will be seen in section 3, in the case of the SiO_2 crystal, three different sets of regions can be suggested; however, the same set of clusters will be used to calculate the LMOs in each case.

2.2. *Localizing functionals*

In a number of methods [24] the localizing functionals are proportional to the non-diagonal electron 'density' associated with region A,

$$\sigma_{\text{A}}(\mathbf{r}, \mathbf{r}') = \sum_{a=1}^{n} \tilde{\varphi}_a(\mathbf{r}) \tilde{\varphi}_a^*(\mathbf{r}') \tag{5}$$

where the summation is performed over all n LMOs of region A. Note that for convenience of the final equations we have omitted a factor of two above as it is unimportant for the eigenproblem (4) to be solved. Therefore, the functionals can be represented in the following general form:

$$\Omega_{\text{A}} = \int [\hat{\Omega}_{\text{A}} \sigma_{\text{A}}(\mathbf{r}, \mathbf{r}')]_{\mathbf{r}' \to \mathbf{r}} \, \mathrm{d}\mathbf{r} = \sum_{a=1}^{n} \int \tilde{\varphi}_a^*(\mathbf{r}) \hat{\Omega}_{\text{A}} \tilde{\varphi}_a(\mathbf{r}) \, \mathrm{d}\mathbf{r} \equiv \sum_{a=1}^{n} \sum_{jk}^{\text{occ}} U_{aj}^* \Omega_{jk}^{\text{A}} U_{ak} \tag{6}$$

where $\hat{\Omega}_{\mathrm{A}}$ is the localization operator and the Hermitian matrix $\mathbf{\Omega}^{\mathrm{A}} = \|\Omega^{\mathrm{A}}_{jk}\|$ can easily be written in terms of the canonical MOs using the definition (1):

$$\Omega^{\mathrm{A}}_{jk} = \langle \varphi^{\mathrm{c}}_j | \hat{\Omega}_{\mathrm{A}} | \varphi^{\mathrm{c}}_k \rangle = \sum_{\mu,\nu} C^{\mathrm{c}*}_{\mu j} C^{\mathrm{c}}_{\nu k} \langle \chi_\mu | \hat{\Omega}_{\mathrm{A}} | \chi_\nu \rangle. \tag{7}$$

For all methods to be considered below both the operator $\hat{\Omega}_{\mathrm{A}}$ and the matrix $\mathbf{\Omega}^{\mathrm{A}}$ do not depend on the LMOs sought for, so that in order to obtain the localized orbitals one has simply to find the eigenvectors of the matrix $\mathbf{\Omega}^{\mathrm{A}}$ using equation (4). Three particular localization methods implemented in this work are considered in the following in more detail. Note that one of the methods (method G) was not considered in [21].

2.2.1. Mulliken's net population (method M). In this method the localization region A is specified by a selection of atomic orbitals (AOs) (e.g. on one or two particular atoms in the unit cell). Then, the net atomic Mulliken's [25] population produced by the LMOs in the selected region is maximized [26, 24, 21]. In this case

$$\Omega^{\mathrm{A}}_{jk} = \sum_{\mu,\nu \in \mathrm{A}} C^{\mathrm{c}*}_{\mu j} S_{\mu\nu} C^{\mathrm{c}}_{\nu k} \tag{8}$$

where $S_{\mu\nu}$ is the overlap integral between two AOs χ_μ and χ_ν. The summation here is performed over AOs which are centred in the chosen region A. This way one can make the LMOs to have a maximum contribution from the specified AOs in region A. Sometimes a different choice of AOs centred on the *same* atoms may lead to physically identical localization; however, this is not the case in general [21]. This method will be referred to as method M.

2.2.2. Mulliken's gross population (method G). If, instead, the Mulliken's gross population on the atoms belonging to region A is maximized, one arrives at the Pipek–Mezey localization scheme [27, 24]. In this case the expression for Ω^{A}_{jk} is very similar to that given by equation (8):

$$\Omega^{\mathrm{A}}_{jk} = \tfrac{1}{2} \sum_{\mu \in \mathrm{A}} \sum_{\nu} \left\{ C^{\mathrm{c}*}_{\mu j} S_{\mu\nu} C^{\mathrm{c}}_{\nu k} + C^{\mathrm{c}*}_{\nu j} S_{\nu\mu} C^{\mathrm{c}}_{\mu k} \right\}. \tag{9}$$

The first summation here is performed over AOs which are centred in the chosen region A and another summation is performed over all AOs. This method will be referred to as method G.

2.2.3. The projection on the atomic subspace (method P). Roby's population maximization [28] gives LMOs for which the projection on the subspace spanned by the basis orbitals centred within the selected region A is a maximum, or is at least stationary [24, 21]. In this method the localization operator $\hat{\Omega}_{\mathrm{A}}$ in equation (6) is chosen in the form of a projection operator, so that

$$\Omega^{\mathrm{A}}_{jk} = \sum_{\lambda,\tau} C^{\mathrm{c}*}_{\lambda j} C^{\mathrm{c}}_{\tau k} \left[\sum_{\mu,\nu \in \mathrm{A}} S_{\lambda\mu} (\mathbf{S}^{-1}_{\mathrm{A}})_{\mu\nu} S_{\nu\tau} \right] \tag{10}$$

where $\mathbf{S}^{-1}_{\mathrm{A}}$ stands for the inverse of the overlap matrix $\mathbf{S}_{\mathrm{A}}$ defined on all AOs $\mu, \nu \in A$. Here the first double summation is performed over all AOs of the system. Note that the idempotent operator $\hat{\Omega}_{\mathrm{A}}$ projects any orbital into a subspace spanned by the AOs associated with region A only. Therefore, by choosing particular AOs (and thus the region) one ensures the maximum overlap of the LMOs with them. It is seen that this method, which will be referred to as method P, although different in implementation, is very similar in spirit to the previous two methods.

2.3. Localization criteria

An application of the various schemes described above results in LMOs which are localized in the 3D space differently. It is therefore useful to have simple criteria which can identify the degree of their localization. Note that each of the localization methods of the previous subsection corresponds to a particular linear combination of the canonical orbitals and thus will result in exactly the same electron density (3) provided, of course, that a sufficiently large cluster has been used in the LMO calculation. We assume in this section that this is always the case.

Three methods will be used to assess the localization of calculated LMOs [21].

2.3.1. Localization index. The first method was proposed by Pipek and Mezey [27] and is based on the calculation of the so-called *localization index*:

$$d_a = \left\{ \sum_{\mathrm{B}} \left[\sum_{\mu \in \mathrm{B}} \sum_{\nu} (\tilde{C}_{\mu a} S_{\mu \nu} \tilde{C}_{\nu a}) \right] \right\}^{-1} \tag{11}$$

where the first summation is run over all atoms B of the entire system. Here the quantity in the square brackets is similar to the diagonal part of the localization operator matrix (9) calculated on real localized orbitals. Qualitatively, the localization index gives the number of atoms on which the orbital $\tilde{\varphi}_a(\mathbf{r})$ is predominantly localized. Therefore for the ionic type of bonding one would expect $d_a \sim 1$, and for a valence LMO describing a covalent bonding $d_a \sim 2$.

2.3.2. Eigenvalues of the overlap matrix. Alternatively, the overlap between LMOs also gives important information about their localization. That is why as the second criterion we shall consider the maximum eigenvalue of the overlap matrix. Note that for periodic structures it is more convenient to use the Fourier transformation of the overlap matrix [29]:

$$S_{ab}(\mathbf{k}) = \sum_{\mathbf{L}} \langle \tilde{\varphi}_a(\mathbf{r}) | \tilde{\varphi}_b(\mathbf{r} - \mathbf{L}) \rangle \mathrm{e}^{\mathrm{i}\mathbf{k}\mathbf{L}} \tag{12}$$

where $\mathbf{k}$ is a point in the Brillouin zone, $\tilde{\varphi}_a(\mathbf{r})$ and $\tilde{\varphi}_b(\mathbf{r})$ are LMOs in the zero (central) elementary unit cell and $\mathbf{L}$ is the lattice translation vector. Note that if any of the eigenvalues, $\lambda(\mathbf{k})$, of the overlap matrix $\mathbf{S} = \|S_{ab}(\mathbf{k})\|$ is found to be larger than 2, it is impossible to obtain the total crystal density in this basis by expanding the inverse of the overlap matrix in equation (3) in powers of the overlap (Löwdin's method; see [29] for a detailed discussion). Therefore, the existence of large eigenvalues of the matrix $\mathbf{S}$ corresponds to a weak localization of the LMOs.

2.3.3. Gap in eigenvalues of the localization problem. The eigenvalues λ_a of the secular problem (4) can also be used to indicate the degree of localization [21]. Indeed, if the localization functional Ω_{A} used is appropriate, then

(i) the chosen n solutions would have close eigenvalues λ_a which correspond to their similar localization in region A, and
(ii) the gap $\Delta\lambda$ in the eigenvalues λ_a between the chosen n and other solutions is considerable, i.e. the other solutions will correspond to much worse localization in region A (see [30]).

Therefore, in order to check the localization of the LMOs, we shall also use the parameter $\Delta\lambda$.

One may assume that better localization will give larger gap value $\Delta\lambda$. In principle, if the given region and the right number of LMOs, n, associated with it, were chosen correctly, one should expect some gap $\Delta\lambda$ in the eigenvalues λ_a.

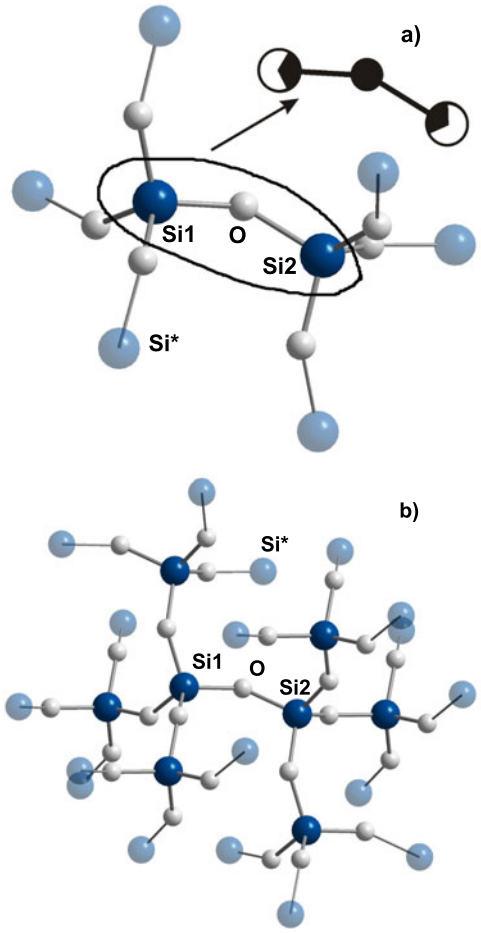

Figure 1. The first two quantum clusters, Si_2O_7 (a) and Si_8O_{25} (b), used in our HF calculations. Point charges surrounding the clusters are not shown. Both silicon atoms (Si1 and Si2) and the oxygen atom of the central unit $Si_{\frac{1}{4}}OSi_{\frac{1}{4}}$ are indicated in each case. The elementary 'brick' the whole system can be composed from is shown schematically in (a).

3. SiO_2 bulk

α-quartz (SiO_2) crystal has a hexagonal Bravais lattice and corresponds to the D_3^4 ($P3_121$, No. 152) space group symmetry [31, 32]. The equilibrium crystal structure has been found using density functional theory, the plane wave basis set, periodic boundary conditions and the method of ultrasoft pseudopotentials as implemented in the VASP code [33–35]. The calculation was carefully converged with respect to the **k** point sampling and the plane wave cut-off. The lattice found is specified by elementary translations $\mathbf{a}_1 = a(0, -1, 0)$, $\mathbf{a}_2 = a(\frac{1}{2}, \frac{\sqrt{3}}{2}, 0)$ and $\mathbf{a}_3 = c(0, 0, 1)$ with $a = 4.913$ Å and $c = 5.4046$ Å. Each cell contains nine atoms distributed over three SiO_2 molecules. Three 3a positions (of local symmetry C_2) are occupied by Si atoms; the position of the first Si atom is given by the fractional coordinates $(-u, -u, \frac{1}{3})$ with $u = 0.4697$; six oxygen atoms occupy the general position 6c, which can be generated from the fractional coordinates (x, y, z) using $x = 0.4135$, $y = 0.2669$ and $z = 0.1191$. The tetrahedron of oxygen atoms with a silicon atom in its centre is almost regular with slightly different Si–O distances of R(Si1–O) = 1.613 Å and R(Si2–O) = 1.604 Å. The whole 3D crystal structure can be constructed from $Si_{\frac{1}{4}}OSi_{\frac{1}{4}}$ units connected together at the Si atoms as shown schematically in figure 1(a). Four such units have a common Si atom at the centre of a tetrahedron, and six complete inequivalent units (positioned differently in space)

form an elementary cell. Note that this is similar to the Si crystal structure where the whole crystal can be composed of $Si_{\frac{1}{4}}Si_{\frac{1}{4}}$ units [21].

Because of such an arrangement of atoms in the α-quartz crystal, it is reasonable to assume that every unit $Si_{\frac{1}{4}}OSi_{\frac{1}{4}}$ forms one independent region. However, as will be shown in the following, one can alternatively consider two or three regions made out of each unit as well. Therefore, in choosing a set of finite clusters, we ensured that the whole $Si_{\frac{1}{4}}OSi_{\frac{1}{4}}$ unit was in the centre of each of the quantum clusters. Three clusters were considered: Si_2O_7, Si_8O_{25} and $Si_{40}O_{103}$, containing 9, 33 and 143 atoms, respectively. The smallest and middle size clusters used are shown in figure 1. To create proper termination of the clusters at their boundary, we implemented special boundary conditions suggested in [15]. In particular, we surrounded clusters by pseudoatoms Si^* which are directly connected to the cluster O atoms. Each Si^* pseudoatom is made of 'classical (3/4th) and 'quantum' (1/4th) parts. The 'classical' part is represented by the electrostatic potential due to a $+1.8e$ point charge (which is a 3/4th of the effective charge on a Si atom in the lattice), e being the elementary charge. The 'quantum' part of the Si^* pseudoatom consists of a central repulsive electronic potential $V(r)$ (added to mimic the screening of the Si core by the valence electrons) and a single valence electron. The parameters of the potential and the basis set for the pseudoatoms were optimized to get proper effective charges on Si and O atoms and to eliminate the contribution of the Si^* electron at the top of the valence and the bottom of the conduction bands. Note that the described boundary conditions were found to be crucial only for the smallest cluster; for the other two clusters simpler boundary conditions (e.g. termination by hydrogen atoms) were also tried and found to give practically identical results for the LMOs and thus will not be discussed further. To simulate the Madelung field, clusters were surrounded by an array of nearly 2.5×10^4 point charges, containing $+2.4e$ charges to mimic Si atoms and $-1.2e$ charges for oxygens.

To simplify the initial HF calculations required to check the convergence of the electron density with the cluster size and generate all occupied canonical molecular orbitals, only valence ($3s^2 3p^2$ on Si and $2s^2 2p^4$ on O) electrons were considered explicitly by using for both species the coreless HF pseudopotentials (CHF) with LP-31G basis set from [36]. The calculations were made with the use of the Gamess-UK package [37].

Figure 2 shows the convergence of the HF electron density with the size of the cluster along the Si1–O direction. We carefully checked, by plotting the densities along other directions and by making 2D plots, that this direction is representative for assessing the convergence in this system. The deep minimum in the density at the oxygen atom is due to the pseudopotential method used. One can see that the difference between curves for the middle sized and the largest clusters is negligible. This suggests that the middle sized cluster Si_8O_{25} is perfectly sufficient for our purposes, and thus it was used in all the calculations described below.

As has been mentioned above, the elementary 'brick' we can build the system from is the unit $Si_{\frac{1}{4}}OSi_{\frac{1}{4}}$ shown in the centre of each of the clusters in figure 1 as an Si1–O–Si2 molecule. Each such unit should be assigned eight electrons in total: six electrons come from the O atom and one electron from each of the two Si atoms. Note that each Si atom contributes to four different units which contain this Si atom. This simple analysis allows us to suggest at least three possible choices (models) for the localization regions:

(i) Each unit $Si_{\frac{1}{4}}OSi_{\frac{1}{4}}$ containing eight electrons is considered as a *single* region; therefore, to obtain the corresponding *four* (doubly occupied) LMOs, one has to choose all AOs centred on the atoms Si1, Si2 and O in the centre of the cluster when applying any of the localizing functionals discussed above. Note that all four LMOs obtained using this partition method will be orthonormal as eigenvectors of the same secular problem (4).

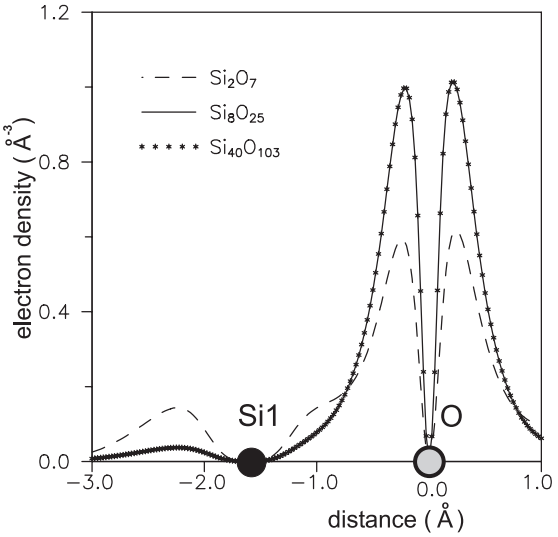

Figure 2. The HF electron densities for the three clusters are plotted along the Si1–O direction. The convergence is obvious: the curves for the middle sized and the largest clusters are indistinguishable.

(ii) Each pair of atoms Si1–O and Si2–O can be considered as a separate region, i.e. there will be *two* regions in total to describe every unit $Si_{\frac{1}{4}}OSi_{\frac{1}{4}}$; four electrons distributed over two (doubly occupied) LMOs will be associated in this case with each of the two regions. Two LMOs associated with either of the two regions will be mutually orthogonal; however, the LMOs belonging to different regions will have a non-zero overlap.

(iii) Finally, each unit can be split into *three* different regions:

(1) the first region, containing two electrons and described by a single LMO, is constructed to describe a covalent bond Si1–O; this can be achieved by enforcing localization on 2p AOs of the O atom and all AOs of the Si1 atom;

(2) the second region is formed similarly to describe the Si2–O bond;

(3) finally, the remaining four electrons are attached to the third region which is localized predominantly on the O atom giving rise to two more (doubly occupied) LMOs; in this case the 2s AOs centred on the O atom can be used to enforce localization. Thus, in this case there will be three sets of the LMOs: two orthogonal LMOs belonging to the O region and another two LMOs belonging to the 'bond' regions; the latter two LMOs have a non-zero overlap with any other LMO.

For each choice of the localization regions described above (which will be referred to as *regions models* hereafter), we can apply either of the three localization methods of section 2 to calculate the LMOs using the obtained occupied canonical orbitals of the middle cluster. When solving the secular problem (4), the contributions of the boundary pseudoatoms Si^* were removed from the canonical orbitals which then were renormalized. Using the obtained LMOs, one should appropriately translate and rotate them in order to obtain all LMOs comprising the whole primitive cell. (For instance, there will be six sets with four LMOs in each in the primitive cell for model 1.) By applying lattice translations to all the LMOs associated with the primitive cell, the whole infinite crystal is reproduced. It is then possible to calculate the total electron density $\rho(\mathbf{r})$ of the whole crystal using equation (3). The necessary lattice summations are handled exactly by converting into $\mathbf{k}$ space [29]. These calculations have been done for all

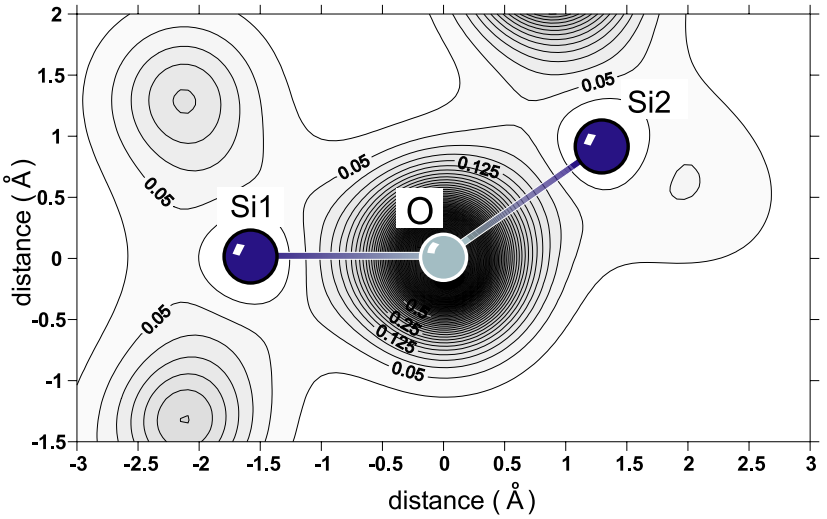

Figure 3. The total electron valence density $\rho(\mathbf{r})$ in the Si1–O–Si2 plane by combining the contributions of LMOs (method M, model 1) across the infinite crystal. The density was calculated using the method [29] based on equation (3).

nine cases (three localization methods versus three choices of the localization regions). The calculated $\rho(\mathbf{r})$ matched exactly the original HF density in the central part of the cluster in all cases, indicating that a very good degree of localization was achieved in each case. As an example, a 2D contour plot of the total valence electron density in the plane of the molecule Si1–O–Si2 calculated using LMOs obtained by method M in model 1 is shown in figure 3. The cross-section of this plot corresponds to a solid curve (the middle cluster) in figure 2. One can see that a considerable amount of the charge is concentrated around oxygen atoms.

The partial region densities, $\rho_{\mathrm{A}}(\mathbf{r}) = \sigma_{\mathrm{A}}(\mathbf{r}, \mathbf{r})$ (see equation (5)), corresponding to each of the regions and generated from the LMOs calculated using method M, are shown in figure 4 as closed 3D surfaces of constant density. The value of the density is chosen in such a way that 90% of the region electron charge is contained inside every surface. In the case of model 1 (the upper panel) only one density is shown; in the case of model 2 (the middle panel) two densities are shown simultaneously, while in the third case (model 3, the bottom panel), all three partial densities are presented. One can see that in the cases of models 2 and 3 the LMOs belonging to neighbouring regions strongly overlap. As was mentioned before, the LMOs belonging to different regions for these two models are not orthogonal. At the same time, the overall shapes of the density for each of the region models are very similar, demonstrating a clear aggregation around the O atom in the middle of the $\mathrm{Si}_{\frac{1}{4}}\mathrm{OSi}_{\frac{1}{4}}$ unit in agreement with the total density shown in figure 3.

A comparison of the LMOs calculated using three localization methods is presented in figure 5 for region model 1. In this figure, the partial densities $\rho_{\mathrm{A}}(r)$ are shown in each case along the Si1–O direction through the $\mathrm{Si}_{\frac{1}{4}}\mathrm{OSi}_{\frac{1}{4}}$ unit. It is clear that the partial density obtained from LMOs calculated using method M is found to be slightly more localized, whereas the localization obtained using method P is slightly worse than that given by the two others. Still, the difference between the densities is extremely small, so we can conclude at this point that all three techniques perform practically equally well (at least for the system under discussion).

The picture becomes more complicated, however, at least at first sight, when the localization criteria of section 2.3 are applied in each of the nine cases as shown in table 1.

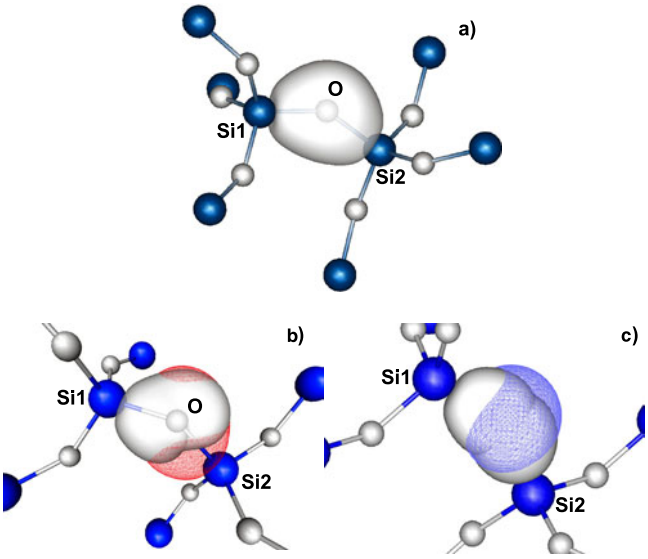

Figure 4. Constant partial density plots for three choices of localization regions: (a) model 1, when the whole unit $Si_{\frac{1}{4}}OSi_{\frac{1}{4}}$ is associated with a single region; (b) model 2, when two regions Si1–O and Si2–O are identified; and (c) model 3, when three regions, Si1–O, Si2–O and O, are identified. In every case the value of the density shown is chosen to enclose 90% of the total electron charge associated with the region. The localization method M was used in each case.

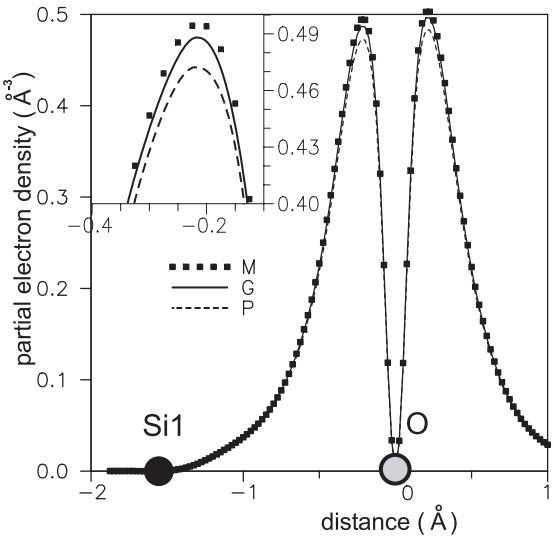

Figure 5. The partial electron density for region model 1 calculated using different localization methods and plotted along the Si1–O direction.

Three groups of rows in this table correspond to the three different choices of localization regions; in each case there are four LMOs in total which are occupied by eight electrons of the elementary $Si_{\frac{1}{4}}OSi_{\frac{1}{4}}$ unit. While the first column is the number of the localization region, the second one shows the centres of localization. The third column corresponds to the indexes

Table 1. Localization criteria calculated for all region models and localization methods.

			Method M			Method G			Method P		
Model	Regions	LMO	d_a	$\max(\lambda(\mathbf{k}))$	$\Delta\lambda$	d_a	$\max(\lambda(\mathbf{k}))$	$\Delta\lambda$	d_a	$\max(\lambda(\mathbf{k}))$	$\Delta\lambda$
1	Si1–O–Si2	1	1.18573			1.20741			1.22195		
		2	1.13868	1.71955	0.92527	1.15423	1.76597	0.77451	1.54019	2.08836	0.30218
		3	1.41971			1.44083			1.17747		
		4	1.12914			1.13788			1.18254		
2	Si1–O	1	1.21753		0.00508	1.20624		0.00223	1.24733		0.00045
		2	1.15569	2.97523		1.17676	2.92854		1.24529	3.07121	
	Si2–O	1	1.20410		0.01659	1.18245		0.00736	1.24529		0.00108
		2	1.16580			1.19308			1.18726		
3	O	1	1.07793		0.06952	1.06777		0.04513	1.11378		0.00112
		2	1.12734	3.43867		1.11958	3.43770		1.12776	3.98629	
	Si1–O	1	1.21753		0.02072	1.20624		0.01363	1.24733		0.00433
	Si2–O	1	1.20410		0.00921	1.18245		0.00868	1.24529		0.00409

of the localization problem solutions (LMO indexes). Then three sets of columns give us the localization criteria values for different methods of localization.

The first criterion (the localization index d_a) is slightly above one in most cases, and is smaller than two in all nine cases. This means that the LMOs are mostly localized on a single atom with some contribution coming from the nearest atoms. However, the maximum eigenvalues of the overlap matrix were found to be below two only for the region model 1 and localization methods M and G; in the cases of models 2 and 3 eigenvalues around three were found, indicating worse localization. Finally, the gap between the eigenvalues of the secular problem of equation (4), $\Delta\lambda$, was found to be too small for the region models 2 and 3, whereas in the case of model 1 and for all three localization methods the gap is considerable, especially for methods M and G. This means that the choice of the regions in models 2 and 3 is somewhat artificial, which is not surprising because of the very strong overlap between LMOs corresponding to the neighbouring regions in these two models.

It follows from this analysis that model 1, in which the whole elementary unit $\mathrm{Si}_{\frac{1}{4}}\mathrm{OSi}_{\frac{1}{4}}$ is considered as one region, results in the best localization of the LMOs, especially if methods M and G are used.

In spite of subtle differences in the applied localization criteria which seem to favour model 1 and methods M and G, we stress that very good localization of the LMOs was obtained in all cases. This conclusion is also supported by an observation that LMOs generated within different models (choices of the regions) span the same Fock space. To make such a conclusion, we calculated the projection of the LMOs of models 2 and 3 on the space spanned by the four orthogonal LMOs obtained in model 1 and then subtracted the projection from the original orbitals. The calculated residual parts were found to be negligible in all cases. Note that this conclusion is not obvious, because each LMO depends on all AOs of the entire cluster.

4. Conclusions

In this paper we have calculated strongly localized molecular orbitals (LMOs) for the SiO_2 crystal (α-quartz) using a method developed earlier [21]. The starting point for the choice of the localization regions was an observation that the whole crystal can be reproduced by rotating and translating a single elementary unit $\mathrm{Si}_{\frac{1}{4}}\mathrm{OSi}_{\frac{1}{4}}$, containing an O atom and *quarters* of the two Si atoms which the O atom is directly connected to. Three localization methods were

applied and three models for choosing the localization regions were tried in each case: (1) the whole unit was considered as one region; (2) the unit was split into two and (3) three regions. Although in all cases well localized orbitals were obtained, we find that the first choice of the localization region, in which the whole unit was chosen as a single region, is preferable.

The LMOs produced in models 2 and 3 were found to be very close to a linear combination of the orthonormal LMOs obtained within model 1. If taken from the nearest regions belonging to the same elementary unit, they appeared to have a significant overlap with each other. On the other hand, the LMOs belonging to different units (in either of the models) do not overlap strongly, which is confirmed by various localization criteria applied in this work and by the corresponding plots of the partial densities.

Since our previous calculations reported in [21] were done for the extreme cases of ionic (MgO) and covalent (Si) bonding, it follows from the results of the present study that our method is also applicable to crystals with intermediate types of chemical bonding.

Note that we did not consider in this study localization method E [21], based on the energy minimization of the structure element corresponding to the chosen region. This is because it was found in [21] that the orbitals obtained by this method for the Si crystal were not sufficiently localized.

Although the LMOs reported in this work may be useful to characterize the chemical bonding in the given crystal, they are needed for the embedding method which is under development. Different possibilities in choosing localization regions open up various ways in terminating the quantum cluster when considering, for example, a point defect in the crystal bulk or an adsorbed species on the crystal surface. This variety of options may be extremely useful in applications to keep the size of the cluster as small as possible. If, for instance, one would like to terminate the cluster with Si atoms, then either of the region models can be used (model 1 would probably be more convenient as the orbitals within each region are orthonormal). However, if a termination with oxygens is required, then region models 2 or 3 may prove to be more useful. In practice, a combination of terminations may be preferable, when both Si and O atoms are used at the boundary. In those cases all three models for choosing localization regions may be employed.

Acknowledgments

OD would like to acknowledge the financial support from the Leverhulme Trust (grant F/07134/S) which has made this work possible. We would also like to thank S Hao for help in the VASP calculations.

References

[1] Sauer J and Sierka M 2000 *J. Comput. Chem.* **21** 1470
[2] Murphy R B, Philipp D M and Freisner R A 2000 *J. Comput. Chem.* **21** 1442
[3] Kantorovich L N 1988 *J. Phys. C: Solid State Phys.* **21** 5041
[4] Kantorovich L N 1988 *J. Phys. C: Solid State Phys.* **21** 5057
[5] Vreven T and Morokuma K 2000 *J. Comput. Chem.* **21** 1419
[6] Abarenkov I V *et al* 1997 *Phys. Rev.* B **56** 1743
[7] Bakowies D and Thiel W 1996 *J. Phys. Chem.* **100** 10580
[8] Hall R J, Hinde S A, Burton N A and Hillier I H 2000 *J. Comput. Chem.* **21** 1433
[9] Assfeld X and Rivail J-L 1996 *Chem. Phys. Lett.* **263** 100
[10] Bredow T 1999 *Int. J. Quantum Chem.* **75** 127
[11] Sushko P V, Shluger A L and Catlow C R A 2000 *Surf. Sci.* **450** 153
[12] Nasluzov V *et al* 2001 *J. Chem. Phys.* **115** 8157
[13] Seijo L S and Barandiaran Z 1996 *Int. J. Quantum Chem.* **60** 617

[14] Erbetta D, Ricci D and Pacchioni G 2000 *J. Chem. Phys.* **113** 10744
[15] Sulimov V, Sushko P, Edwards A, Shluger A and Stoneham A 2002 *Phys. Rev.* B **66** 024108
[16] Kantorovich L N and Zapol B P 1992 *J. Chem. Phys.* **96** 8420
[17] Kantorovich L N and Zapol B P 1992 *J. Chem. Phys.* **96** 8427
[18] Shidlovskaya E K 2002 *Int. J. Quantum Chem.* **89** 349
[19] Fornili A, Sironi M and Raimondi M 2003 *J. Mol. Struct. (Theochem)* **632** 157
[20] Mo Y and Gao J 2000 *J. Comput. Chem.* **21** 1458
[21] Danyliv O and Kantorovich L 2004 *Phys. Rev.* B **70** 075113
[22] Dovesi R *et al* 1998 *CRYSTAL98 User's Manual* (Torino: University of Torino)
[23] McWeeny R 1992 *Methods of Molecular Quantum Mechanics* (London: Academic)
[24] Mayer I 1996 *J. Phys. Chem.* **100** 6249
[25] Mulliken R S 1949 *J. Chem. Phys.* **49** 497
[26] Magnasco V and Perico A 1967 *J. Chem. Phys.* **47** 971
[27] Pipek J and Mezey P G 1989 *J. Chem. Phys.* **90** 4916
[28] Roby K 1974 *Mol. Phys.* **27** 81
[29] Danyliv O and Kantorovich L 2004 *J. Phys.: Condens. Matter* **16** 2575
[30] Whitten J L and Pakkanen T A 1980 *Phys. Rev.* B **21** 4357
[31] Wyckoff R W G 1963 *Crystal Structures* 2nd edn (New York: Wiley)
[32] Kantorovich L 2004 *Quantum Theory of the Solid State: An Introduction* (*Fundamental Theories of Physics*) (Dordrecht: Kluwer–Academic)
[33] Kresse G and Furthmüller J 1996 *Comput. Mater. Sci.* **6** 15
[34] Kresse G and Furthmüller J 1996 *Phys. Rev.* B **54** 11169
[35] Kresse G and Hafner J 1994 *J. Phys.: Condens. Matter* **6** 8245
[36] Melius C and Goddard W III 1974 *Phys. Rev.* A **10** 1528
[37] Guest M F *et al* 1980 *GAMESS-UK, A Package of Ab Initio Programs* NRCC software catalog, vol 1, program no. qg01 ed